

Clara Bionda · Xing Jun Li · Robin van Bruggen ·
Michel Eppink · Dirk Roos · Françoise Morel ·
Marie-José Stasia

Functional analysis of two-amino acid substitutions in *gp91phox* in a patient with X-linked flavocytochrome *b₅₅₈*-positive chronic granulomatous disease by means of transgenic PLB-985 cells

Received: 8 April 2004 / Accepted: 29 June 2004 / Published online: 24 August 2004
© Springer-Verlag 2004

Abstract Chronic granulomatous disease (CGD) is a rare inherited disorder in which phagocytes lack NADPH oxidase activity. The most common form is caused by mutations in the *CYBB* gene encoding *gp91phox* protein, the heavy chain of cytochrome *b₅₅₈*, which is the redox element of NADPH oxidase. In some rare cases, the mutated *gp91phox* is normally expressed but no NADPH oxidase can be detected. This type of CGD is called X91⁺ CGD. We have previously reported an X⁺ CGD case with a double-missense mutation in *gp91phox*. Transgenic PLB-985 cells have now been made to study the impact of each single mutation on oxidase activity and assembly to rule out a possible new polymorphism in the *CYBB* gene. The His303Asn/Pro304Arg *gp91phox* transgenic PLB-985 cells exactly mimic the phenotype of the neutrophils of the X⁺ CGD patient. The His303Asn mutation is sufficient to inhibit oxidase activity in intact cells and in a broken cell system, whereas in the Pro304Arg mutant, residual activity suggests that the Pro304Arg substitution is less devastating to oxidase activity than the His303Asn mutation. The study of NADPH oxidase assembly following the in vitro and in vivo translocation of cytosolic factors *p47phox* and *p67phox* has demonstrated that, in the double mutant and in the His303Asn mutant, NADPH oxidase assembly

is abolished, although the translocation is only attenuated in Pro304Arg mutant cells. Thus, even though the His303Asn mutation has a more severe inhibitory effect on NADPH oxidase activity and assembly than the Pro304Arg mutation, neither mutation can be considered as a polymorphism.

Introduction

The dysfunction of NADPH oxidase in phagocytes results in a severe orphan genetic disease, chronic granulomatous disease (CGD). Patients with CGD suffer from recurrent, often life-threatening, bacterial and fungal infections because of the absence of a superoxide anion (O₂⁻) - generating system (Winkelstein et al. 2000). NADPH oxidase is a multi-component complex composed of membrane-bound cytochrome *b₅₅₈*, the cytosolic proteins *p67phox*, *p47phox*, *p40phox* and two small GTPases, Rac2 and Rap1A. Cytochrome *b₅₅₈*, the redox center of the NADPH oxidase complex, is a heterodimer consisting of a large flavocytochrome *gp91phox* (or β sub-unit or Nox2) and a small protein *p22phox* (or α sub-unit). In resting cells, cytosolic and membrane-bound components of the NADPH oxidase complex are dissociated. During the activation of phagocytotic cells by several activators, such as the C5a complement fragment, cytokines, chemotactic peptides, opsonized bacteria or fungi, the NADPH oxidase complex becomes assembled and the activated enzyme can produce bactericidal O₂⁻ (Vignais 2002).

The three types of autosomal CGD exhibit mutations in the genes encoding the *p47phox*, *p67phox* and *p22phox* proteins, whereas the most common X-linked CGD type (approximately 60%) has defects in the *CYBB* gene encoding *gp91phox* in which cytochrome *b₅₅₈* is absent (X91⁰; Segal et al. 2000). The *CYBB* gene (GenBank accession no. X04011) was one of the first to be identified by positional cloning (Royer-Pokora et al. 1986), following chromosomal localization to Xp21.1 (Baehner et al. 1986). It encompasses 13 exons spanning about 30 kb

Clara Bionda and Xing Jun Li contributed equally to this work

C. Bionda · X. J. Li · F. Morel · M.-J. Stasia (✉)
GREPI EA 2938, Lab Enzymologie, CHU,
38043, Grenoble Cedex 9,
France
e-mail: MJStasia@chu-grenoble.fr
Tel.: +33-476-765483
Fax: +33-476-765608

R. van Bruggen · D. Roos
Sanquin Research at CLB and Landsteiner Laboratory,
Academic Medical Centre, University of Amsterdam,
1066 CX Amsterdam, The Netherlands

M. Eppink
Diosynth BV,
5340 BH Oss, The Netherlands

genomic DNA (Skalnik et al. 1991). In the majority of X-linked CGD cases, mutations, including deletions, insertions, splice site, missense and nonsense mutations, lead to an unstable gp91*phox* protein with either absent or markedly reduced expression (Roos et al. 1996). The *CYBB* gene appears to be extremely sensitive to mutations because only one polymorphism within the coding region has been discovered (Kuribayashi et al. 1996). In a few rare cases, missense mutations resulting in normal levels of nonfunctional cytochrome *b*₅₅₈ have been identified (X91⁺; for a review, see Heyworth et al. 2003). Some of these have provided interesting information about the structure of NADPH oxidase and its activation mechanisms (Cross et al. 1995; Leusen et al. 1994, 2000). An in vitro cellular model of X-CGD has been developed (Zhen et al. 1993). The X chromosome-linked CGD locus is disrupted by homologous recombination in the PLB-985 human myeloid cell line (X-CGD PLB-985 cells). Only one functional analysis of an X⁺ CGD case has been studied in these transgenic cells (Yu et al. 1999). An X⁺ CGD patient with a double mutation (C919A and C923G, leading to His303Asn/Pro304Arg substitution) close to the putative flavin adenine dinucleotide (FAD)-binding site in gp91*phox* has been previously reported (Stasia et al. 2002). However, FAD binding is normal but NADPH oxidase assembly is strongly inhibited during the in vitro activation process. A double-mutation is a rare event in genetic diseases and determination of the real disease-causing mutation is generally difficult, especially in the case of a missense type. Generally, a single base change is sufficient to provoke the disease. Only one double missense mutation has been reported in the *NCF2* gene encoding p67*phox* resulting in CGD disease (Bonizzato et al. 1997).

In the present study, we stably transfected the His303Asn, the Pro304Arg or the double substitution gp91*phox* cDNA into X-CGD PLB-985 cells to create cell lines expressing the first, second or double-gp91*phox* mutation. The control cell line was the X-CGD PLB-985 cells transfected with the wild-type (WT) gp91*phox* cDNA (WT gp91*phox* cDNA PLB-985 cells) in which the NADPH oxidase was totally restored. The aim was carefully to dissect the impact of each mutation and the double mutation on gp91*phox* expression and on the activity and assembly of NADPH oxidase and to rule out the eventuality of a new polymorphism in the *CYBB* gene.

Gene symbols used in this article follow the recommendations of the HUGO Gene Nomenclature Committee (Povey et al. 2001)

Materials and methods

Construction of transgenic PLB-985 cell lines

His303Asn, Pro304Arg and the double mutation were generated from the WT gp91*phox* cDNA in pBlue-ScriptKS(+) vector by site-directed mutagenesis (Quik change site-directed mutagenesis kit, Stratagene, La Jolla,

Calif., USA). The WT and the mutated gp91*phox* cDNA were sub-cloned into the *Bam*H1 site of the mammalian expression vector pEF-PGKneo (a generous gift from Dr. M. C. Dinauer). The insertion sense and the gp91*phox* cDNA sequence mutation were verified by sequencing (Genome Express, Grenoble, France) on the Abi Prism automatic sequencer (Perkin Elmer, Courtaboeuf, France). All the gp91*phox* cDNA constructs were transfected into X-CGD PLB-985 cells (provided by Dr. M. C. Dinauer) by electroporation at 250 V (one pulse of 20 ms). Positive clones were selected by limited dilution in the presence of 1.5 mg/ml Geneticin.

Cell culture and granulocyte differentiation

Wild-type, X-CGD and transfected PLB-985 cells (expressing WT or the mutant gp91*phox* in His303Asn, Pro304Arg or double mutants) were maintained in RPMI-1640 supplemented with 10% (vol/vol) fetal calf serum, 100 U/ml penicillin, 50 µg/ml streptomycin, 2 mM L-glutamine at 37°C in a 5% CO₂ atmosphere. In transgenic PLB-985 cells after selection, 0.5 mg/ml Geneticin was added to maintain the selection pressure. To induce differentiation and expression of endogenous NADPH oxidase components, cells were differentiated for 6 days with 0.5% (vol/vol) dimethylformamide (DMF; Tucker et al. 1987). The WT PLB-985 cells are the original WT PLB-985 cells; the X-CGD PLB-985 cells are WT PLB-985 cells in which the *CYBB* gene had been knock-out; the WT gp91*phox* PLB-985 cells were X-CGD PLB-985 cells transfected with WT gp91*phox* cDNA; the His303Asn or Pro304Arg or His303Asn/Pro304Arg gp91*phox* PLB-985 cells were X-CGD PLB-985 cells transfected with the His303Asn or Pro304Arg or His303Asn/Pro304Arg mutated gp91*phox* cDNA.

Assessment of gp91*phox* protein expression by flow cytometry

Gp91*phox* expression in transgenic and WT PLB-985 cells was assessed by using monoclonal antibodies (mAbs) directed against an external epitope of gp91*phox* (7D5; Yamauchi et al. 2001) or control monoclonal IgG1 (Immunotech, Marseille, France) as described in Stasia et al. (2003). Results are expressed as mean fluorescence intensity (MFI) values in arbitrary units (au). All experiments were performed in triplicate.

Chemiluminescent detection of H₂O₂ production

H₂O₂ production of intact granulocyte-differentiated cells (5×10⁵ cells) in phosphate-buffered saline (PBS) containing 20 mM glucose, 10 U/ml horseradish peroxidase, 0.02 mM luminol were stimulated with 80 ng/ml phorbol myristate acetate (PMA; Dahlgren and Karlsson 1999). Relative luminescence unit (RLU) counts monitored at

37°C were estimated in a Luminoscan luminometer (Labsystems, Helsinki, Finland) coupled to a computer.

Cytochrome *b*₅₅₈ spectroscopy

Purified neutrophils treated with 3 mM diisopropyl fluorophosphate were lysed for cytochrome *b*₅₅₈ extraction. The supernatant was used for the immunoblotting experiment and cytochrome *b*₅₅₈ spectroscopy. Reduced minus oxidized differential absorption spectra were recorded at room temperature on a DU 640 Beckman spectrophotometer (Batot et al. 1998).

SDS-polyacrylamide gel electrophoresis and immunoblotting

Proteins solubilized in a 1% Triton X100 from neutrophils were separated by SDS-polyacrylamide gel electrophoresis (SDS-PAGE) in 10% (wt/vol) acrylamide gel with a 5% (wt/vol) stacking gel (Laemmli 1970), electrotransferred to nitrocellulose (Towbin et al. 1979), and immunodetected by mAbs 449 and 48 directed against p22*phox* and gp91*phox*, respectively (Verhoeven et al. 1989).

Cell-free superoxide-generating system

NADPH oxidase activity was reconstituted through a broken cell system (BCS). Briefly, neutrophil membranes (30 µg) were mixed with cytosol (300 µg) in PBS buffer containing 20 µM GTPγS, 5 mM MgCl₂ and arachidonic acid in a final volume of 100 µl. After incubation, the oxidase was measured in the presence of 100 µM cytochrome *c* with 150 µM NADPH (Cohen-Tanugi et al. 1991).

In vitro cytosolic proteins p47*phox* and p67*phox* translocation in a BCS

Translocation of cytosolic factors p47*phox* and p67*phox* to the plasma membranes after in vitro NADPH oxidase activation was performed following classical procedures (Stasia et al. 2002).

In vivo p47*phox* translocation by confocal microscopy analysis

Differentiated PLB-985 cells (10⁶) in 10 mM HEPES pH 7.4 (138 mM NaCl, 2.7 mM KCl, 8.1 mM Na₂HPO₄, 1.5 mM KH₂PO₄, 0.6 mM CaCl₂, 1.0 mM MgCl₂, 5.5 mM glucose, and 0.5% (wt/vol) human albumin) deposited on coverslips were activated for 10 min or 30 min with serum-treated zymosan (STZ; 0.2 mg/ml) at 37°C. The cells were washed with PBS, fixed and permeabilized with methanol and incubated for 1 h at room temperature with a

mAb directed against p47*phox* (a generous gift from Dr. Heyworth). The cells were then stained with Alexa-568-labelled goat-anti-mouse-Ig antibodies (Molecular Probes, Eugene, Ore., USA). After a 1-h incubation, the cells were washed twice with PBS. The p47*phox* localization in STZ-treated PLB-985 cells was examined with a Zeiss Axiovert 100 confocal laser-scanning microscope and analyzed with LSM 5 software (Zeiss, Göttingen, Germany).

Ribbon diagram of the three-dimensional model of the cytosolic part of gp91*phox*

With the program SwissPDB Viewer, a picture of the three-dimensional (3D) model of gp91*phox* was made and the residues His303 and Pro304 were highlighted (Taylor et al. 1993; Guex and Peitsch 1997).

Protein determination

Protein content was estimated by using the Bradford assay (Bradford 1976) or the Pierce method (Smith et al. 1985).

Results

Gp91*phox* expression in transgenic PLB-985 cells that mimicked X⁺ CGD neutrophils

A high stable expression of recombinant His303Asn/Pro304Arg, His303Asn and Pro304Arg gp91*phox* in X-CGD PLB-985 cells was observed by flow cytometry after staining with the 7D5 mAb recognizing an external epitope of gp91*phox* (Fig. 1A). The specificity of the 7D5 binding was assessed with an irrelevant monoclonal IgG1. Gp91*phox* expression was as high in the WT gp91*phox* PLB-985 cells as in the double-mutant cells. The level of recombinant His303Asn or Pro304Arg gp91*phox* protein assessed by MFI values in Table 1 was slightly less than in the double-mutant transgenic PLB-985 cells. In contrast, in X-CGD PLB-985 cells transfected with the empty vector pEF-PGKneo, gp91*phox* at the cellular membrane was undetectable. Nevertheless, the high gp91*phox* expression in transgenic PLB-985 cells was confirmed by semi-quantitative immunoblotting analysis. P22*phox* expression was higher in WT or mutated gp91*phox* PLB-985 cells than in X-CGD PLB-985 cells (Fig. 1B). Other clones containing the studied mutations (ten clones for His303Asn gp91*phox* PLB-985 cells, ten clones for Pro304Arg gp91*phox* PLB-985 cells, and six clones for His303Asn/Pro304Arg gp91*phox* PLB-985 cells) were also tested for their expression of gp91*phox*. Similar levels of mutated recombinant protein were observed for each type of mutant cell (data not shown). Reduced-minus-oxidized difference spectra were performed in 1% Triton-X100 soluble extracts from transfected PLB-985 cells. Identical spectra characteristic of flavocytochrome *b*₅₅₈ were observed for both mutated

and WT *gp91phox* PLB-985 cells and the amount of cytochrome *b₅₅₈* correlated with the level of *gp91phox* expression checked by flow cytometry (Table 1, Fig. 1C). Thus, the expression of recombinant WT or mutated *gp91phox* was efficient in transgenic PLB-985 cells and the methods used, viz. flow cytometry, Western blot and spectrophotometry, gave similar results for the quantification of the level of *gp91phox* expression.

The NADPH oxidase activity in transfected X-CGD PLB-985 cells

The functional analysis of WT *gp91phox* PLB-985 cells was performed to check whether our tools and methodology to restore oxidase activity were efficient (ex vivo therapy). We first examined respiratory-burst oxidase activity in intact transgenic PLB-985 cells expressing recombinant WT *gp91phox* by means of the chemiluminescence technique to measure H_2O_2 formation quantitatively after PMA stimulation. At least six different types of clone for each studied mutation were tested for their

NADPH oxidase activity in intact cells, giving similar results (data not shown). With granulocytic differentiation in 0.5% DMF, H_2O_2 production from WT *gp91phox* PLB-985 cells was comparable with the activity measured in the original WT PLB-985 cells with a maximum at day 6 (Fig. 2). In His303Asn/Pro304Arg *gp91phox* PLB-985 cells, NADPH oxidase activity was totally abolished. The His303Asn mutation was sufficient totally to inhibit the respiratory burst of transgenic PLB-985 cells and the inhibitory effect was independent of the time of differentiation (Fig. 2). In the Pro304Arg *gp91phox* PLB-985 cells, very low NADPH oxidase activity was measured, corresponding to about 4% of the activity found in control WT *gp91phox* PLB-985 cells, as seen in the insert of Fig. 2. Individually, both mutations had an inhibitory effect on NADPH oxidase activity but the impact of the His303Asn substitution was apparently more pronounced than that of the Pro304Arg mutation in intact transgenic PLB-985 cells.

The NADPH oxidase activity was then studied in an in vitro O_2^- -generating system (BCS) by using purified plasma membranes from all transgenic PLB-985 cells. In

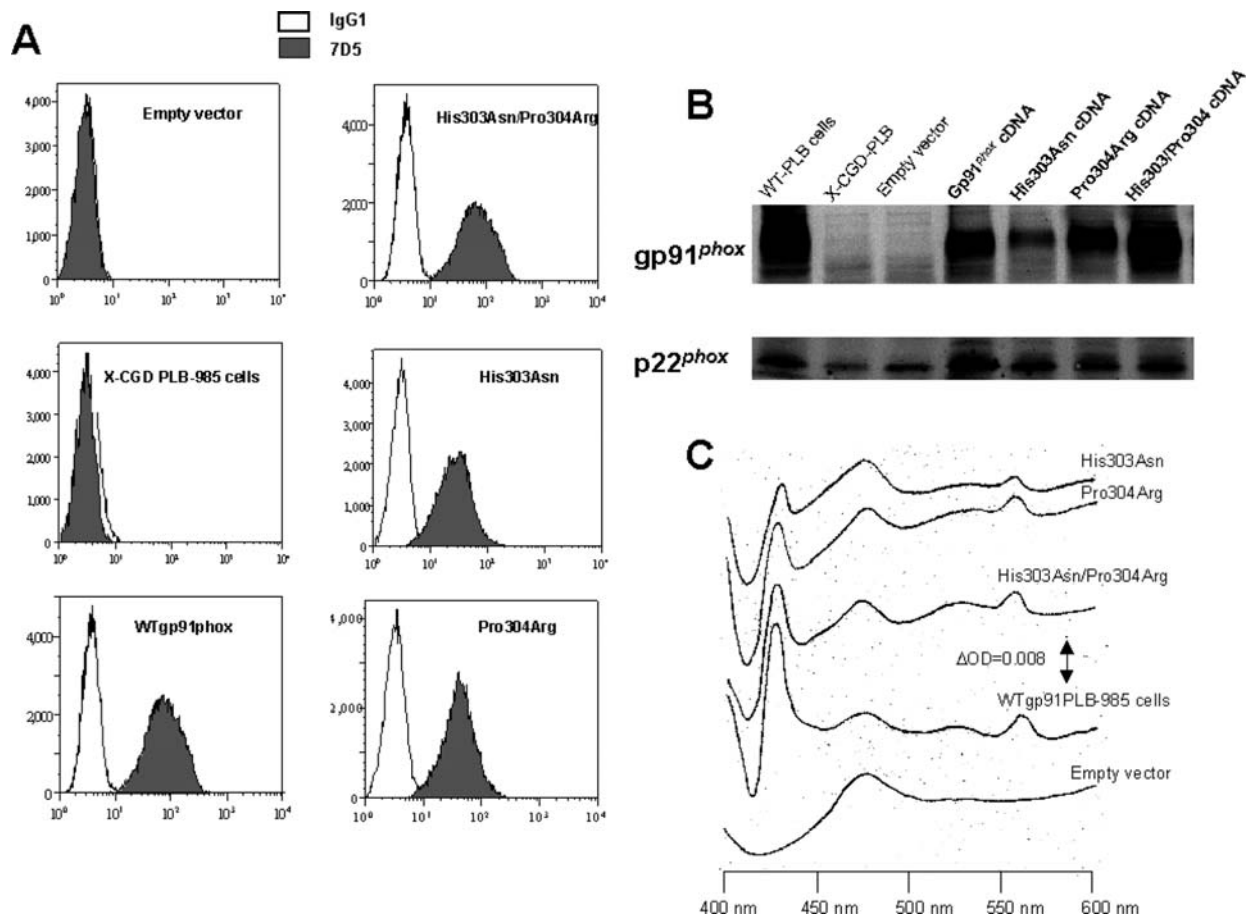


Fig. 1A–C Expression of recombinant WT and mutated *gp91phox* in transgenic PLB-985 cells. **A** Transgenic PLB-985 cells (5×10^5) were incubated with the *gp91phox* mAb 7D5, as described. Mouse IgG1 isotype was used as an irrelevant mAb. **B** Immunodetection of *p22phox* and *gp91phox* sub-units of cytochrome *b₅₅₈* was performed with 50 μ g 1% Triton-X100 soluble extracts subjected to SDS-

PAGE (10% acrylamide gel), blotted onto a nitrocellulose sheet and revealed with mAbs 449 and 48. **C** Cytochrome *b₅₅₈* differential spectra of transgenic PLB-985 cells were conducted with the same soluble extract of transgenic PLB-985 cells as described in **B**. Results are from one representative from triplicate analyses

Table 1 Phenotypic characterization of transgenic PLB-985 cells. (MFI mean fluorescence intensity in au). Haem content was quantified by the Soret absorption of 1% Triton-X100 soluble extract from transgenic cells, considering that cytochrome b_{558} contains two haems. H_2O_2 production was measured by chemiluminescence from 5×10^5 intact transgenic PLB-985 cells differentiated with 0.5% DMF for 6 days and stimulated with 80 ng/ml PMA. Relative luminescence unit (RLU) represents the sum of RLU

Transgenic PLB-985 cells	Gp91 <i>phox</i> expression MFI (au)	Cytochrome b_{558} pmol/mg proteins	H_2O_2 production RLU	Percentage of control	O_2^- production in a BCS assay (nmol/min/mg) protein	Percentage of control
X-CGD PLB-985 cells	3	0	0.6±0.1	0	7.1±3.8	4
Empty vector	3	0	0.5±0.1	0	10.7±5.0	6
His303Asn gp91 <i>phox</i>	32	10.4±2.4	0.6±0.1	0	37.8±15.3	22
Pro304Arg gp91 <i>phox</i>	49	14.2±0.2	17.7±4.7	4	115.3±17.9	67
His303/Pro304 gp91 <i>phox</i>	84	24.2±0.5	0.5±0.1	0	41.7±28.9	24
WTgp91 <i>phox</i>	90	21.8±0.7	362.4±15.5	99	147.7±11.9	86
WT PLB-985 cells (control)	95	26.3±3.0	364.9±10.6	100	170.8±3.4	100

measured over 1.5 h. NADPH oxidase activity was reconstituted in a CFS assay with purified plasma membranes of the indicated cells (30 µg) in the presence of neutrophil cytosol (300 µg) and activated with GTPγS and arachidonic acid. O_2^- was measured by the SOD-sensitive cytochrome *c* reduction assay. Values in the table represent the mean ± SD of triplicate determinations

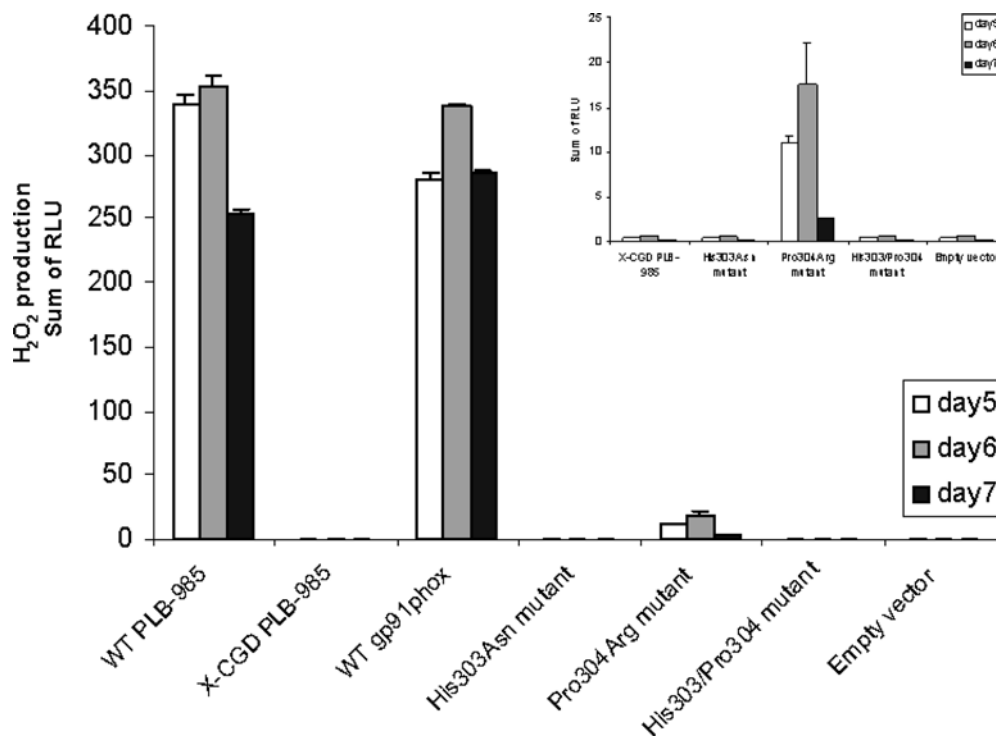
order to compare only the effect of mutations on gp91*phox* in the plasma membranes, cytosol from purified human neutrophils was used as a source of cytosolic NADPH oxidase components. The in vitro oxidase activity in WT gp91*phox* PLB-985 cells was nearly identical to that of the WT PLB-985 cells (Table 1). Residual NADPH oxidase activity was measured in the double-mutant cells and in the His303Asn gp91*phox* PLB-985 cells (24% and 22% of the WT PLB-985 cell activity, respectively). In contrast, Pro304Arg gp91*phox* PLB-985 cells exhibited about 60% of the WT gp91*phox* PLB-985 cells reconstituted oxidase activity. This confirmed that the Pro304Arg mutation had less effect on NADPH oxidase activity than the His303Asn substitution and that the amount of Pro304Arg

gp91*phox* was sufficient to reconstitute a part of the NADPH oxidase activity in a BCS.

Study of the assembly of the NADPH oxidase complex in transgenic PLB-985 cells

In a previous publication, we demonstrated that the His303Asn/Pro304Arg mutation of the gp91*phox* protein in neutrophils of a X^+ CGD patient inhibit the in vitro translocation of the cytosolic factors p47*phox* and p67*phox* to the plasma membrane disturbing the NADPH oxidase assembly (Stasia et al. 2002). Here, the aim was to determine whether the inhibitory effect of each

Fig. 2 NADPH oxidase activity in whole transgenic PLB-985 cells during the time course of differentiation. The indicated cells were induced for granulocytic differentiation with 0.5% DMF. H_2O_2 production by whole intact cells was measured on days 5, 6, and 7 by chemiluminescence by using luminol in the presence of peroxidase. *Insert* Magnification of some results from Fig. 2. Results represent the mean ± SD of triplicate determinations



single mutation and the double mutation on NADPH oxidase activity was related to a defect of its assembly in vitro and in vivo. As seen in Fig. 3A, in WT *gp91phox* PLB-985 cells, the translocation of *p47phox* and *p67phox* to the plasma membranes occurs normally as observed for WT PLB-985 cells and for human control neutrophils. In addition, as we had previously observed in neutrophils of the X⁺ CGD patient, no translocation of the cytosolic factors was detected when the plasma membranes originated from the His303Asn/Pro304Arg *gp91phox* PLB-985 cells. For the single mutation, a faint cytosolic factor translocation was shown (more visible for *p47phox*) but the defect of translocation was more pronounced for the His303Asn than for the Pro304Arg mutation. No in vitro cytosolic factor translocation to the plasma membrane was visible after SDS and GTP γ S stimulation in the

X-CGD PLB-985 cells transfected with the empty vector (data not shown) or in human neutrophils from an X⁰ CGD patient (Fig. 3A). This confirmed that, in the absence of cytochrome *b₅₅₈*, no translocation of *p67phox* and *p47phox* could occur.

Then the in vivo *p47phox* translocation was checked in WT, X-CGD and transgenic PLB-985 cells differentiated for 6 days with 0.5% DMF and stimulated in the presence of STZ for 10 or 30 min at 37°C. The assembly of the oxidase complex was evaluated by confocal microscopy to follow the *p47phox* translocation to the phagosomal membranes (Fig. 3B). Undisturbed phagocytosis of STZ was checked by phase contrast microscopy. In the original X-CGD PLB-985 cells transfected with the empty vector pEF-PGKneo, phagocytosis of STZ occurred even in the absence of *gp91phox* and NADPH oxidase activity but

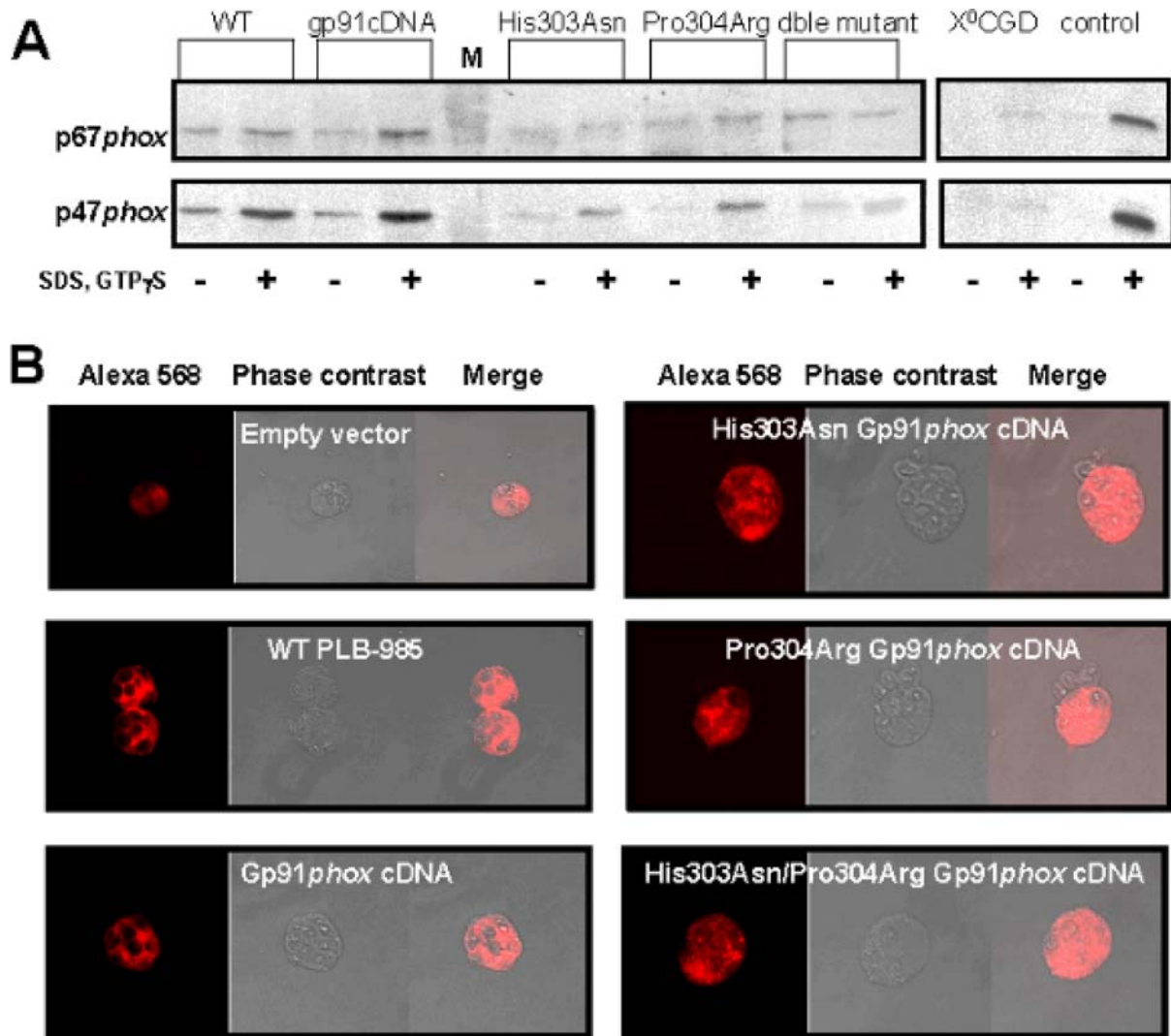


Fig. 3A, B Study of the NADPH oxidase assembly in transgenic PLB-985 cells. **A** NADPH oxidase was activated in vitro in the presence (+) or absence (-) of SDS and GTP γ S in human neutrophil cytosol, by using purified membrane fractions from transgenic PLB-985 cells, human control neutrophils and neutrophils from a X⁰ CGD patient. *p47phox* and *p67phox* were detected in plasma membranes by Western blot after purification in a discontinuous

sucrose gradient. This result represents one experiment of three. **B** In vivo *p47phox* translocation was followed in STZ-activated transgenic PLB-985 cells by confocal microscopy analysis. A total of 10⁶ WT PLB-985 cells or X-CGD PLB-985 cells or the indicated transgenic PLB-985 cells were stimulated with STZ for 10 min on day 6 after DMF differentiation

p47 $phox$ was uniformly distributed in the cytosol indicating that there was no translocation to the membrane of the phagosome. In contrast, in WT gp91 $phox$ PLB-985 cells, p47 $phox$ translocation occurred, as a strong red fluorescence was seen surrounding the STZ particles. On the contrary, no p47 $phox$ translocation was observed in the double-mutant gp91 $phox$ PLB-985 cells or in His303Asn gp91 $phox$ PLB-985 cells. However, in Pro304Arg gp91 $phox$ PLB-985 cells, the p47 $phox$ translocation occurred but with a seemingly lower efficiency than in WT 91 $phox$ PLB-985 cells. The same results were obtained in a second set of experiments in which the incubation time of transgenic PLB-985 cells with STZ was 30 min instead of 10 min (data not shown). We concluded that the double-mutated gp91 $phox$ PLB-985 cells exactly mimicked the phenotype of the X⁺ CGD neutrophils previously described. The absence of NADPH oxidase activity was thus related to a defect in oxidase component assembly during *in vitro* and *in vivo* activation. The single mutation His303Asn also induced the inhibition of this assembly, whereas Pro304Arg had a weak effect upon it related to the remaining oxidase activity measured in Pro304Arg mutant PLB-985 cells.

The functional significance of the His303Asn and Pro304Arg mutation was further analysed in a 3D-model of the C-terminal tail of gp91 $phox$ (Taylor et al. 1993; Leusen et al. 2000). This model shows that both His303 and Pro304 are located at the surface of the protein, at the N-terminal of the beta-sheet (β F2) in hydrophilic surroundings (Fig. 4). The charge changes induced by the mutations (His303Asn, more neutral; Pro304Arg, strongly positive) will therefore not strongly affect the positions of the surrounding residues. Moreover, His303 and Pro304 do not form strong hydrogen bonds with nearby amino acids and do not directly interact with FAD or NADPH (the distance is minimally 6–7 Å).

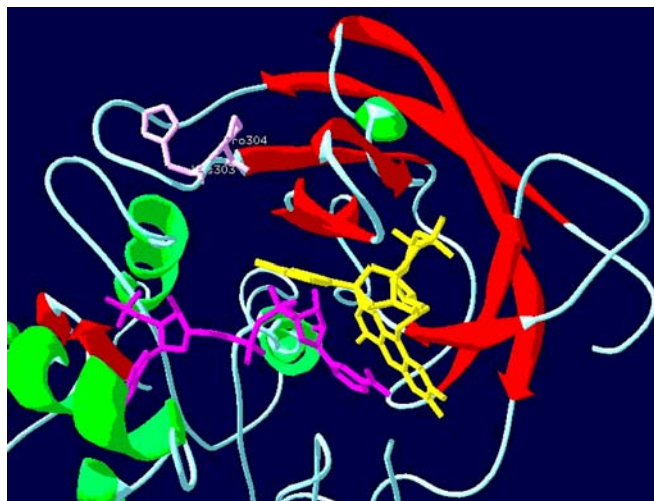


Fig. 4 Ribbon diagram of the 3D-model of the cytosolic C-terminal tail of gp91 $phox$ with the specific residues His303 and Pro 304 located in the ribbon structure. The α -helices are depicted as cylinders and the β -sheets as arrows. His303 and Pro304 are indicated in pink, the FAD cofactor in yellow and the coenzyme NADPH in purple

Discussion

The neutrophil respiratory-burst dysfunction resulting from an X⁺ CGD double-missense mutation was recently reported (Stasia et al. 2002). Here, transgenic X-CGD PLB-985 cells have been used to investigate the impact of His303Asn and/or Pro304Arg mutations and to correlate these mutations with NADPH oxidase assembly and activity. This approach has also been effective in ruling out the possibility of a new polymorphism in the *CYBB* gene.

Cell therapy strategy in X-CGD PLB-985 cells

The first step of our approach was to validate our methodology and tools for restoring NADPH oxidase activity in the X-CGD PLB-985 cells transfected with the WT gp91 $phox$ cDNA (*ex vivo* therapy; Zhen et al. 1993; Yu et al. 1999). A high level of WT recombinant gp91 $phox$ protein appeared to be correctly processed and targeted to the plasma membrane (Fig. 1A), because the 7D5 monoclonal Ab recognized an external epitope of gp91 $phox$ (Yamauchi et al. 2001). There was a good correlation between the level of gp91 $phox$ expression in transgenic WT gp91 $phox$ PLB-985 cells checked by flow cytometry, Western blot analysis and differential spectrophotometry (Table 1, Fig. 1A–C). The last-mentioned method demonstrated normal haem group incorporation in the recombinant gp91 $phox$ protein. An increase in p22 $phox$ expression in transgenic PLB-985 cells versus X-CGD PLB-985 cells was consistent with previous observations, indicating that the co-expression of both sub-units of cytochrome b_{558} and heterodimer synthesis was essential for the stable expression of the haemoprotein (DeLeo et al. 2001). NADPH oxidase activity in WT gp91 $phox$ PLB-985 cells was restored in a similar range to that originally measured in differentiated WT PLB-985 cells (Fig. 2, Table 1). All these results established that the cultured myeloid PLB-985 cell line genetically deficient in gp91 $phox$ was a useful tool for expressing recombinant gp91 $phox$ for functional analysis, as previously described in a similar approach (Yu et al. 1999).

The second step was to investigate the phenotype of the X⁺ CGD mutations (His303Asn/Pro304Arg) after transfection of each mutated cDNA or both in X-CGD PLB-985 cells. As shown in Table 1 and Fig. 1, lower levels of cytochrome b_{558} were detected in single mutated gp91 $phox$ PLB-985 cells than in the double-mutant cells, whereas recombinant mutated gp91 $phox$ proteins were correctly processed. This was observed in other tested clones for each type of mutation. Possibly, the double mutation provided greater translation efficiency than did the single mutation. This was shown previously, the authors demonstrating that the functional correction of X-CGD neutrophils did not require a high level of gp91 $phox$ (Zhen et al. 1993). The double mutation His303Asn/Pro304Arg led to total inhibition of the oxidase activity in whole transgenic PLB-985 cells, independently of the

differentiation day (Fig. 2). Surprisingly, the His303Asn substitution was sufficient to abolish NADPH oxidase activity entirely, although residual activity was measured with the second mutation Pro304Arg. After oxidase reconstitution in the BCS, the His303Asn mutation had the same inhibitory effect on oxidase activity as the double mutation (Table 1), whereas Pro304Arg gp91*phox* PLB-985 cells showed roughly 60% of the reconstituted oxidase activity of WT gp91*phox* PLB-985 cells. The Pro304Arg mutation had a lower effect on NADPH oxidase activity in intact cells and particularly in BCS than did the His303Asn mutation; artificial NADPH oxidase assembly in vitro is probably not completely comparable to that in vivo. For example, NADPH oxidase activity can be reconstituted in vitro in the absence of p47*phox* and in the presence of a large amount of p67*phox* (Paclet et al. 2000). The arachidonic acid may change the conformation of proteins and force cytosolic factor interactions within cytochrome *b*₅₅₈. In contrast, in AR47⁰ CGD cases with the absence of p47*phox*, no oxidase activity can be measured in the neutrophils of the patients.

In a previous article characterizing the studied double-missense mutation in two first cousins suffering from an X⁺ CGD (Stasia et al. 2002), no double or single mutations were found in genomic DNA purified from 50 healthy donors (50% were women). We conclude that the phenotype of the His303Asn/Pro304Arg gp91*phox* PLB-985 cells exactly mimics that of the neutrophils of the X⁺ CGD patient and that neither mutation can be considered as a polymorphism in the *CYBB* gene.

Only one polymorphism has been described in the *CYBB* gene (G1102C); this predicts a Gly364Arg substitution that neither affects NADPH oxidase activity nor gp91*phox* expression (Kuribayashi et al. 1996). Thus, the *CYBB* gene appears to be highly sensitive to mutations. Another striking point is that a double-missense mutation is a rare event in human diseases. Generally, a single base change is sufficient to induce a genetic illness. For example, in cystic fibrosis, which is the most common genetic disease, no double-missense mutations have been found in the 532 reported cases in the human gene mutation database (Stenson et al. 2003). In addition, the reported double-mutation cases often involve two missense mutations localized in the same allele but not close to each other (Yamamoto et al. 1998; Saad et al. 1998). In CGD disease, only one case of a double-missense mutation has been reported in the *NCF2* gene, the patient being heterozygous for each mutation according to genomic DNA analysis (Bonizzato et al. 1997). However, a double-missense mutation D2625E/A2626P has been found in the ATM protein of a Dutch family with ataxia telangiectasia (Van Belzen et al. 1998); this results in a change in the secondary structure of the mutated ATM protein (the effect of each single mutation was not studied). To our knowledge, our study is the first to report a double-missense mutation in a human genetic disease in detail following the use of direct mutagenesis and transfection experiments in a human cell line.

A number of single nucleotide substitution mechanisms have been identified (Cooper and Krawczak 1990). The best known is point mutation via methylation-mediated deamination, CG dinucleotides indeed being hotspots of mutation causing human genetic diseases. The C-to-A and C-to-G substitutions found in our case have not frequently been described and may be caused by polymerase-mediated misincorporation of bases during DNA replication, perhaps by a mechanism involving transient base misalignment. The probability that both missense mutations occurred at the same time is very weak. Interestingly, Pro304 is highly preserved in gp91*phox* analogues in plants (Torres et al. 1998) and in microorganisms (Lalucque and Silar 2003), whereas His303 and Pro304 appear in *Dictyostelium Discoideum* (Genbank accession no. AY221173). His303 and Pro304 seem to play an important role in the NAD(P)H oxidase activity in eukaryotic cells because they are preserved in all Nox analogues except His 303 in Nox 5 (Cheng et al. 2001).

NADPH oxidase assembly

The 3D-model of the C-terminal tail of gp91*phox* (Fig. 4) highlights the localization of His303 and Pro304 at the surface of gp91*phox* and indicates that the distance to the FAD-binding site is not compatible with a direct interaction of these amino acids with the binding site. This confirms our previous result that FAD binding is not affected by the double mutation (Stasia et al. 2002). We show in the present paper, both in vitro and in vivo, that both His303Asn and Pro304Arg mutations, separately and together, are correlated with the dysfunction of cytosolic factor translocation. Moreover, the level of resulting oxidase activity is proportional to the extent of translocation efficiency (Fig. 3, Table 1). The strongest effect on the structure of the protein might be expected from the Pro304Arg mutation, because this affects the backbone of the loop between β F1 and β F2 and might have an effect on the binding sites for p47*phox* and p67*phox*, probably located at the surface of the protein. Nevertheless, the net charge of this loop region is probably important for p47*phox* binding and NADPH oxidase activity.

The main conclusion of the present work is the validation of the X⁺ CGD transgenic PLB-985 cellular model for efficiently studying the functional consequences of the double and single mutations His303/Pro304 on NADPH oxidase activation and assembly. Double-mutated gp91*phox* transgenic PLB-985 cells exactly mimic the phenotype of the X⁺ CGD neutrophils previously described, in which the absence of NADPH oxidase activity is related to a defect in oxidase complex assembly. Our results also suggest that the His303Asn mutation is sufficient to prevent NADPH oxidase activity and assembly, whereas the Pro304Arg substitution has less effect on it, but neither mutation can be considered as a polymorphism.

Nevertheless, we have not established that His303 and Pro304 directly bind p47*phox* and/or p67*phox*. The

mutations may lead to a conformational change in cytochrome *b*₅₅₈ disturbing cytosolic factor assembly. The conformational change in mutated cytochrome *b*₅₅₈ and its direct interaction with cytosolic factors are currently under investigation in our laboratory by atomic force microscopy (Paquet et al. 2000) with a simplified activation system including purified mutated cytochrome *b*₅₅₈ and recombinant p47*phox* and/or p67*phox* proteins.

Acknowledgements We are grateful to Dr. Mary C. Dinauer for the generous gift of X-CGD PLB-985 cells and for critical reading of the manuscript and helpful suggestions. We thank Dr. François Boulay and Dr. Marie Josephe Rabiet for their judicious advice in transfection experiments. The 7D5 and the mAb against p47*phox* were generous gifts from Dr. Michio Nakamura and Dr. Paul G. Heyworth, respectively. We also thank Ms. Linda Northrup for correction of the English. This work was supported by grants from the Université Joseph Fourier, Faculté de Médecine; the Région Rhône-Alpes, programme Emergence; the Ministère de l'Éducation et de la Recherche; MENRT; and the Direction de la Recherche Régionale Clinique, DRRC.

References

- Baehner RL, Kundel LM, Monaco AP, Haines JL, Conneally PM, Palmer C, Heerema N, Orkin SH (1986) DNA linkage analysis of X chromosome-linked chronic granulomatous disease. *Proc Natl Acad Sci USA* 83:3398–3401
- Batot G, Paquet MH, Doussière J, Vergnaud S, Martel C, Vignais PV, Morel F (1998) Biochemical and immunochemical properties of B lymphocyte cytochrome *b*₅₅₈. *Biochim Biophys Acta* 1406:188–202
- Bonizzato A, Russo MP, Donini M, Dusi S (1997) Identification of a double mutation (D160 V-K161E) in the p67*phox* gene of a chronic granulomatous disease patient. *Biochem Biophys Res Commun* 231:861–863
- Bradford MM (1976) A rapid and sensitive method for quantitation of microgram quantities of protein utilizing the principle of protein-dye binding. *Anal Biochem* 72:248–254
- Cheng G, Cao Z, Xu X, Meir EG van, Lambeth JD (2001) Homologs of gp91*phox*: cloning and tissue expression of Nox3, Nox4, and Nox5. *Gene* 269:131–140
- Cohen-Tanugi L, Morel F, Pilloud-Dagher MC, Seigneurin JM, François P, Bost M, Vignais PV (1991) Activation of O₂⁻ generating oxidase in heterologous cell-free system derived from Epstein-Barr-virus-transformed human B lymphocytes and bovine neutrophils. *Eur J Biochem* 202:649–655
- Cooper DN, Krawczak M (1990) The mutational spectrum of single base-pair substitutions causing human genetic disease: patterns and predictions. *Hum Genet* 85:55–74
- Cross AR, Heyworth PG, Rae J, Curnutte JT (1995) A variant X-linked chronic granulomatous disease patient (X91⁺) with partially functional cytochrome *b*. *J Biol Chem* 270:8194–8200
- Dahlgren C, Karlsson A (1999) Respiratory burst in human neutrophils. *J Immunol Methods* 232:3–14
- DeLeo FR, Burritt JB, Lixin Y, Jesaitis AJ, Dinauer MC, Nauseef W (2001) Processing and maturation of flavocytochrome *b*₅₅₈ include incorporation of heme as a prerequisite for heterodimer assembly. *J Biol Chem* 275:13986–13993
- Guex N, Peitsch MC (1997) Swiss-model and the Swiss-PdbViewer: an environment for comparative protein modeling. *Electrophoresis* 18:2714–2723
- Heyworth PG, Cross AR, Curnutte JT (2003) Chronic granulomatous disease. *Curr Opin Immunol* 15:578–584
- Kuribayashi F, Boer M de, Leusen JH, Verhoeven AJ, Roos D (1996) A novel polymorphism in the coding region of CYBB the human gp91-*phox* gene. *Hum Genet* 97:611–613
- Laemmli UK (1970) Cleavage of structural proteins during the assembly of the head of bacteriophage T4. *Nature* 227:680–685
- Lalucque H, Silar P (2003) NADPH oxidase: an enzyme for multicellularity? *Trends Microbiol* 11:9–12
- Leusen JHW, Boer M de, Bolscher GJM, Hilarius PM, Weening RS, Ochs HD, Roos D, Verhoeven AJ (1994) A point mutation in gp91-*phox* of cytochrome *b*₅₅₈ of the human NADPH oxidase leading to defective translocation of the cytosolic proteins p47-*phox* and p67-*phox*. *J Clin Invest* 93:2120–2126
- Leusen JHW, Meischl C, Eppink MHM, Hilarius PM, Boer M de, Weening RS, Ahlin A, Sanders L, Goldblatt D, Skopczynska H, Bernatowska E, Palmblad J, Verhoeven AJ, Berkel WJH van, Roos D (2000) Four novel mutations in the gene encoding gp91-*phox* of human NADPH oxidase: consequences for oxidase assembly. *Blood* 95:666–673
- Paquet MH, Coleman AW, Vergnaud S, Morel F (2000) P67-*phox* mediated NADPH oxidase assembly: imaging of cytochrome *b*₅₅₈ liposomes by atomic force microscopy. *Biochemistry* 39:9302–9310
- Povey S, Lovering R, Bruford E, Wright M, Lush M, Wain H (2001) The Hugo Gene Nomenclature Committee (HGNC). *Hum Genet* 109:678–680
- Roos D, Boer M de, Kuribayashi F, Meischl C, Weening RS, Segal AW, Ahlin A, Nemet K, Hossle JP, Bertatowska-Matuskiewicz E, Middleton-Price H (1996) Mutations in the X-linked and autosomal recessive forms of chronic granulomatous disease. *Blood* 87:1663–1681
- Royer-Pokora B, Kundel LM, Monaco AP, Goff SC, Newburger PE, Baehner RL, Cole FS, Curnutte JT, Orkin SH (1986) Cloning the gene for an inherited disorder-chronic granulomatous disease-on the basis of its chromosomal localisation. *Nature* 322:32–38
- Saad FA, Merlini L, Mostacciolo ML, Danieli GA (1998) Double missense mutation in exon 41 of the human dystrophin gene detected by double strand conformation analysis. *Am J Med Genet* 80:99–102
- Segal BM, Leto TL, Gallin JI, Malech HL, Holland SM (2000) Genetic, biochemical, and clinical features of chronic granulomatous disease. *Medicine (Baltimore)* 79:170–200
- Skalnik DG, Strauss EC, Orkin SH (1991) CCAAT displacement protein as a repressor of the myelomonocytic-specific gp91-*phox* gene promoter. *J Biol Chem* 266:16736–16744
- Smith PK, Krohn RI, Hermanson GT, Mallia AK, Gartner FH, Provenzano MD, Fujimoto EK, Goeke NM, Olson BJ, Klenk DC (1985) Measurement of protein using bicinchoninic acid. *Anal Biochem* 150:76–85
- Stasia MJ, Lardy B, Maturana A, Rousseau P, Martel C, Bordigoni P, Demarex N, Morel F (2002) Molecular and functional characterization of a new X-linked chronic granulomatous disease variant (X91⁺) case with a double missense mutation in the gp91-*phox*-cytosolic C-terminal tail. *Biochem Biophys Acta* 1586:316–330
- Stasia MJ, Brion JP, Boutonnet J, Morel F (2003) Severe clinical forms of cytochrome *b*-negative chronic granulomatous disease (X91⁻) in three children with point mutation in the promoter region of the *CYBB* gene. *J Infect Dis* 188:1593–1604
- Stenson PD, Ball EV, Mort M, Phillips AD, Shiel JA, Thomas NS, Abeyasinghe S, Krawczak M, Cooper DN (2003) Human gene mutation database (HGMD). *Hum Mutat* 21:577–581
- Taylor WR, Jones DT, Segal AW (1993) A structural model for the nucleotide binding domains of the flavocytochrome *b*-245 *b*-chain. *Protein Sci* 2:1675–1685
- Torres MA, Onouchi H, Hamada S, Machida C, Hammond-Kosack KE, Jones JDG (1998) Six *Arabidopsis thaliana* homologues of the human respiratory burst oxidase (gp91-*phox*). *Plant J* 14:365–370
- Towbin H, Staehelin T, Gordon J (1979) Electrophoretic transfer of proteins from polyacrylamide gels to nitrocellulose sheets: procedure and some application. *Proc Natl Acad Sci USA* 76:4350–4354

- Tucker KA, Lilly MB, Heck L Jr, Rado TA (1987) Characterization of a new human diploid myeloid leukemia cell line (PLB-985) with granulocytic and monocytic differentiating capacity. *Blood* 70:372–378
- Van Belzen MJ, Hiel JA, Weemaes CM, Gabreels FJ, Engelen BG van, Smeets DF, Heuvel LP van den (1998) A double missense mutation in the ATM gene of a Dutch family with ataxia telangiectasia. *Hum Genet* 102:187–191
- Verhoeven AJ, Bolscher GJM, Meerhof L, Zwieter R van, Keijer J, Weening RS, Roos D (1989) Characterization of two monoclonal antibodies against cytochrome *b*₅₅₈ of human neutrophils. *Blood* 73:1686–1694
- Vignais PV (2002) The superoxide-generating NADPH oxidase: structural aspects and activation mechanism. *Cell Mol Life Sci* 59:1428–1459
- Winkelstein JA, Marino MC, Johnston RB Jr, Boyle J, Curnutte J, Gallin JI, Malech HL, Holland SM, Ochs H, Quie P, Buckley RH, Foster CB, Chanock SJ, Dickler H (2000) Chronic granulomatous disease. Report on a national registry of 368 patients. *Medicine (Baltimore)* 79:155–169
- Yamamoto K, Sato H, Fujiyama Y, Doida Y, Bamba T (1998) Contribution of two missense mutations (G71R and Y486D) of the bilirubin UDP glycosyltransferase (UGT1A1) gene to phenotypes of Gilbert's syndrome and Criggle Najjar syndrome type II. *Biochim Biophys Acta* 1406:267–273
- Yamauchi A, Yu L, Potgens AJ, Kuribayashi F, Nunoi H, Kanegasaki S, Roos D, Malech HL, Dinauer MC, Nakamura M (2001) Location of the epitope for 7D5, a monoclonal antibody raised against human flavocytochrome *b*₅₅₈, to the extracellular peptide portion of primate gp91phox. *Microbiol Immunol* 45:249–257
- Yu L, Cross AR, Zhen L, Dinauer MC (1999) Functional analysis of NADPH oxidase in granulocytic cells expressing a Δ 488–497 gp91-phox deletion mutant. *Blood* 94:2497–2504
- Zhen L, King AA, Xiao Y, Chanock SJ, Orkin SH, Dinauer MC (1993) Gene targeting of X chromosome-linked chronic granulomatous disease locus in a human myeloid leukemia cell line and rescue by expression of recombinant gp91-phox. *Proc Natl Acad Sci USA* 90:9832–9836